Hindawi
Geofluids
Volume 2023, Article ID 3996378, 12 pages
https://doi.org/10.1155/2023/3996378

Research Article

Study the Elastic Parameters of Sandy Conglomerate under Different Burial History and Petrophysical Modeling

Bin Wang[1], **Jianguo Pan**[2], **Yu Huang**[2], **Guodong Wang**[2], **Yongqiang Qu**[2], **and Jianguo Zhao**[1]

[1]*State Key Laboratory of Petroleum Resource and Prospecting, China University of Petroleum (Beijing), Beijing, China*
[2]*PetroChina Research Institute of Petroleum Exploration and Development, Gansu, China*

Correspondence should be addressed to Bin Wang; owen0104@126.com and Jianguo Zhao; zhaojg@cup.edu.cn

Received 22 September 2022; Revised 19 December 2022; Accepted 19 January 2023; Published 15 February 2023

Academic Editor: Yingfang Zhou

Over the past few years, significant exploration breakthroughs have been made in the sandy conglomerates reservoir of the Triassic Baikouquan Formation in the Mahu Sag, Junggar Basin, China. However, the elasticity and pore characteristics of the tight sandy conglomerates reservoir in this area are still unclear. Through a systematic sonic testing program of the sandy conglomerates sample collected from the Mahu Sag, the regularity behind the variation of the elasticity and pore characteristics of the sample has been analyzed and captured. The Triassic Baikouquan Formation of the slope of Mahu Sag has been through complex burial and diagenetic history. The compaction, cementation, and dissolution are the three types of diagenesis that have the greatest impact on pore characteristics in the study area. In order to quantitatively describe the influence of this complex burial and diagenetic history, we present a rock-physics modeling approach to describe the elastic properties of sandy conglomerate sample. The overall strategy of the modeling is to combine the contact cement theory (CCT), differential effective medium (DEM) and the upper Hashin-Shtrikman bound. The CCT model can well describe the history of cementation, DEM model is suitable for the history of dissolution, and HS upper bound is used to describe the history of compaction. Then, the model is used to describe well log data from sandy conglomerates reservoirs in Mahu Sag and successfully explain the rock porosity, pore shape trends, and the elasticity in the sandy conglomerate reservoirs.

1. Introduction

The Junggar Basin located in northwestern China is a typical superimposed hydrocarbon-bearing basin, with sandy conglomerates reservoirs extensively developed in the Mahu Sag of the northwestern margin of the basin [1–3]. Over the recent years, exploration breakthroughs have been successively made in the Lower Triassic Baikouquan Formation and Upper Permian Upper Wuerhe Formation of the slope-depression area of the Mahu Sag [4–6]. The Baikouquan oil reservoir in the slope area of the Mahu Sag is developed in the sandy conglomerate formation of the underwater distributary channel facies of the fan delta. The oil reservoir boundary is mainly controlled by the quality of the sandy conglomerates reservoir, and the varied diagenesis resulted from the difference in the feldspar content of the sandy conglomerates, palaeogeotemperature, and formation fluid is the fundamental contributor to the reservoir quality variation [7–11].

In terms of the current exploration of subtle reservoirs in the graben basin, the exploration of the sandy conglomerate rock body located in the steep slope of the graben basin has attracted increasing attention from the hydrocarbon explorer [12, 13]. In particular, the sandy conglomerate rock body proximally deposited in the lacustrine source rock system of the steep slope of the graben basin, which favors the hydrocarbon accumulation and storage, has become one of the key oil and gas reservoir exploration and evaluation targets. The Shengli oilfield has made considerable achievements with respect to the sandy conglomerate oil reservoir exploration and development, and substantial progresses have been found in understanding of the genetic type,

sedimentary characteristic and pattern, reservoir characteristic and control factor, favorable reservoir identification and predication, oil and gas accumulation, and so on [14, 15].

Understanding the seismic properties of the low porosity sandy conglomerates is essential for improved quantitative analysis and interpretation of the reservoir quality of the Mahu Sag. The sandstones have generally undergone severe mechanical and geochemical compaction processes that cause a large reduction in their original porosity from the time of their deposition. For quantitative analysis, the effect of different diagenesis on porosity, many scientists have carried out theoretical simulation of petrophysics. Dvorkin et al. combine the contact cement model with effective medium theory to capture the transition from 0% to 100% cement concentration [16]. Berryman uses the DEM model to describe the relationship between porosity and elastic parameters during rock dissolution [17]. Wyllie et al. and Lei et al. use a time-average formula to show the results of the relationship between porosity and velocity during the rock burial [18]. Avseth et al. and Yu et al. present a new rock-physics modeling approach to describe the elastic properties of low-to-intermediate-porosity sandstones that incorporates the depositional and burial history of the rock [19]. Owing to the lack of systematic theoretical and experimental study of the correlation between the reservoir characteristic parameters and the seismic parameter response, especially the insufficient understanding of the correspondence between the terrestrial sandy conglomerate seismic elastic characteristics and the specific sedimentary and diagenetic environments and processes, one has failed to construct a systematic characteristic response pattern of the rock seismic elasticity to the corresponding sedimentary and diagenetic process of the sandy conglomerates reservoir. This, to a great extent, impacts and restrains the accuracy of the seismic reservoir prediction and evaluation of the tight sandy conglomerate reservoir in the Mahu Sag. Given the aforementioned, this paper systematically carried out a seismic petrophysical study with respect to the sedimentary and diagenetic evolution of the sandy conglomerates reservoir, identified the relationship between the reservoir rock status and the physical mechanism of the seismic elastic property variation of such reservoirs during the sedimentary and diagenesis processes, and successfully built a quantitative seismic petrophysical response model to characterize the specific sedimentary and diagenetic evolution processes.

2. Geological Background and Reservoir Lithological Feature

The Mahu Sag located in the northwestern margin of the Junggar Basin is adjacent to the well-known thrust fault zone also in the northwestern margin of the basin (Figure 1(b)). The NE-SW trending depression is an intracontinental depression, generally dipping toward SW (accordingly the depth of the Baikouquan Formation is gradually increasing from west to east and ranges from 2800 m to 4400 m). Local low-amplitude anticlines or nose-like structures are found, and faults are well developed [20–22]. Due to the adjacency of the Mahu Sag to the northwest-margin thrust fault zone, its structural and sedimentary evolution is also generally controlled by the northwest-margin thrust fault zone. The Lower Triassic Baikouquan Formation overrides the boundary uplift originated from the obduction in the Late Hercynian, with great piedmont subsidence magnitudes and thick sedimentation, and the alluvial fan-fan delta proximal coarse-clastic sedimentary system is extensively developed in the slope-depression area [23, 24].

The rock samples used in this research all come from the clastic rock of the Triassic Baikouquan Formation in the Mahu Sag. To investigate the effects of diagenesis in such tight sands on the elastic parameter variations, over 40 samples are used to characterize the seismic elastic characteristics of the rock. A set of gravity-flow coarse-clastic fan delta sedimentary system is developed in the Baikouquan Formation in the slope of the Mahu Sag, and besides the conventional sedimentary facies such as the underwater distributary channel, gravity-flow sedimentary facies such as the mud debris flow and fine-gravel grain flow. The extensive brown silty mudstone of the interchannel flooding and relatively rare dark gray shallow-lake mudstone are found between the fan sandy conglomerates bodies, which indicates the water of the fan sedimentation is shallow. Depending on the sedimentary setting, the rock lithology in the study area can be further divided into 11 types, including above-water mud-debris-flow muddy conglomerate, braided channel sandy conglomerates, and interchannel flooding mud of the fan delta plain; underwater main channel conglomerate and sandy conglomerate, underwater distributary channel sand and pebbly sand, underwater mud debris flow muddy conglomerate, under water grain-flow sandy fine gravel, and mouth bar-distal bar medium-fine-grained sandy conglomerates of the fan delta front; and siltstone and mudstone of the fan delta front. Reservoirs mainly occur in the underwater distributary channel sandy conglomerates and pebbly sandy conglomerates and underwater grain-flow sandy fine gravel of the fan delta front and the braided channel sandy conglomerates of the fan delta plain.

In terms of the rock composition of the tested samples, the volumetric faction of quartz ranges from 24% to 50%, averaging 37%; feldspar ranges from 17% to 52%, with an average of 32%; lithic fragment, 42%~59%, averaging 51%. The rock classification is shown in Figure 2. The rock is seen with middle textural maturity, with average clay contents of 4.3% and high clay contents in local areas up to 20%, which indicates the characteristics of mud debris flow sedimentation of the alluvial fan. The average cement content is 2.6%. The sorting is middle-low, and the psephicity is rounded-subangular and subrounded-angular. The contact between grains is characterized by point-line and line-line, while the cementation type is porous-contact-type and embedded-porous-type.

3. Diagenesis and Their Types in Reservoirs of the Mahu Sag

Diagenesis plays a vital role in the formation, evolution, maintaining, and destruction of the reservoir pore, and a decisive role, in terms of the reservoir physical property.

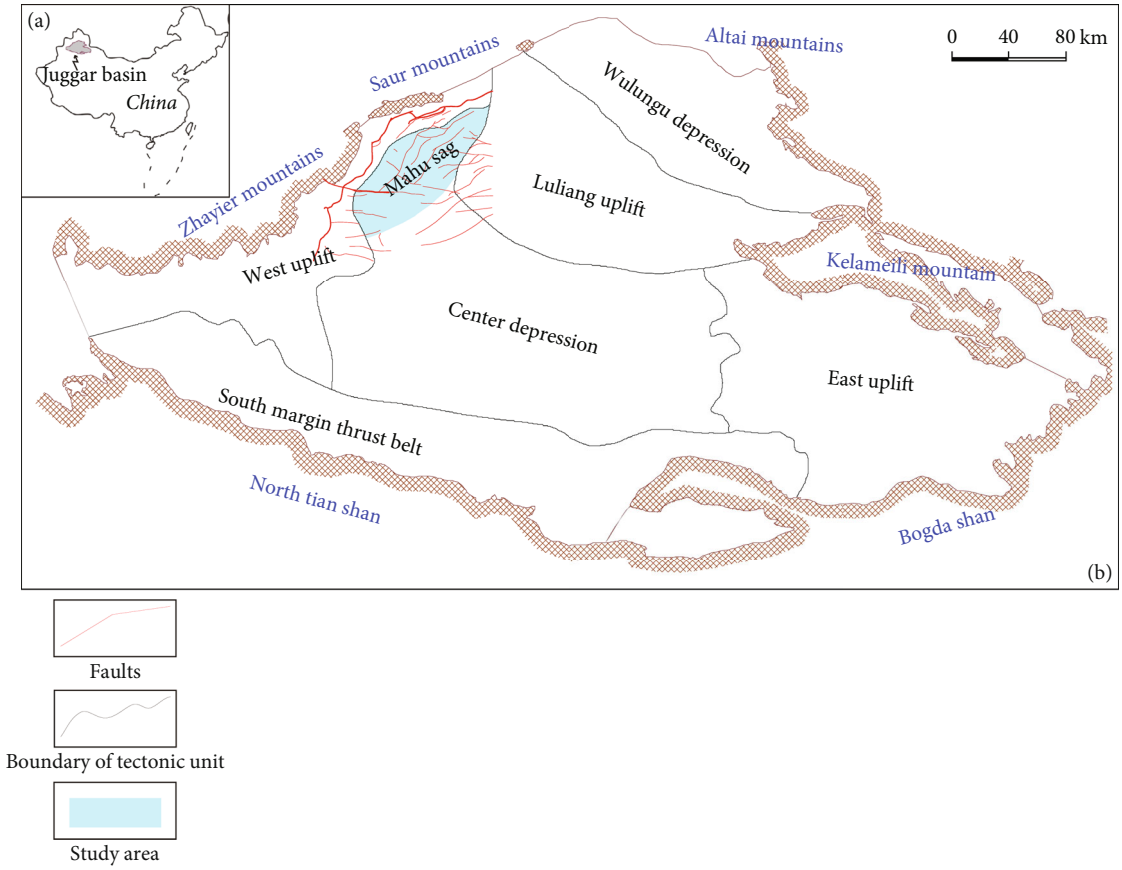

Figure 1: (a) Shows the location of the Junggar Basin in China; (b) shows the structure units around and the internal units in the Junggar Basin.

The Triassic Baikouquan Formation of the Mahu Sag has been through complex diagenetic processes, which mainly include compaction, cementation, and dissolution, with minor recrystallization and replacement.

3.1. Compaction. Compaction, including the mechanical compaction, chemical compaction, and pressure solution, has apparent negative impacts upon the reservoir physical property. Under the microscope, it is observed that the plastic grains (e.g., lithics of mica, shale, and volcanic rocks) tend to bend under the strong compaction stress, and part of the plastic grains bended under pressures fill in the pores and throats, forming the pseudomatrix (Figure 3(a)). The compaction intensifies, with the increasing depth of the sandy conglomerates, which results in the tight directional arrangement of the clastic grains (Figure 3(b)). Rigid grains (e.g., quartz and feldspar particles) break under pressures, and the feldspar often splits along the cleavage crack. As the compaction further grows, the point contact of the grains evolves into the line-contact, concave-convex-contact, and ultimately suture-contact due to pressure solution, after which the reservoir property further deteriorates.

The compaction, a diagenetic process with the strongest negative effects upon the reservoir physical property of the study area, leads to massive loss of the primary porosity, which is also irreversible. Besides the burial depth, the compaction is also related to the compositional and textural

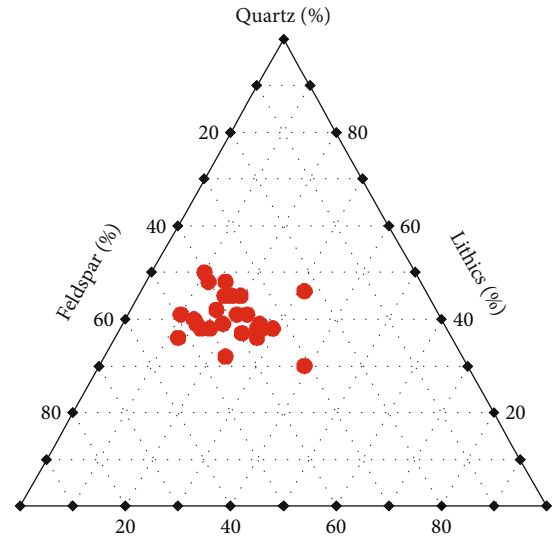

Figure 2: Rock classification of rock samples from the slope of Mahu Sag.

maturity of the sandy conglomerates. The compositional maturity of the Triassic Baikouquan Formation in the Mahu Sag is relatively low, with less quartz that is resistant to compaction and more semiplastic and plastic particles that are relatively vulnerable in terms of compaction. The sandy conglomerate composition has a strong tendency to deform

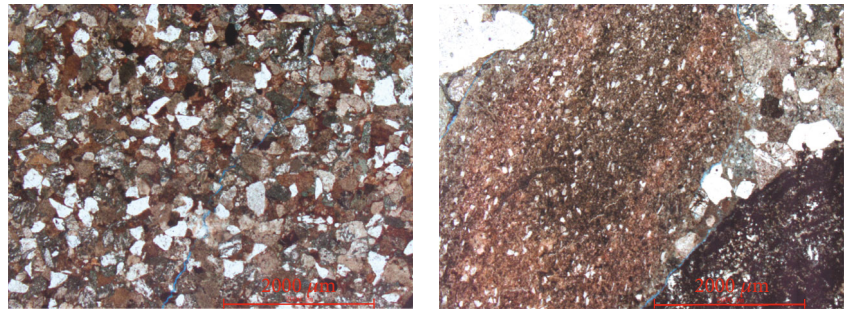

(a) (b)

Figure 3: Thin-section observation of compaction features of sandy conglomerates from Triassic Baikouquan Formation in the slope of the Mahu Sag. (a) Pseudomatrix formed by plastic grains deformed under pressure and (b) tight directional arrangement of plastic grains.

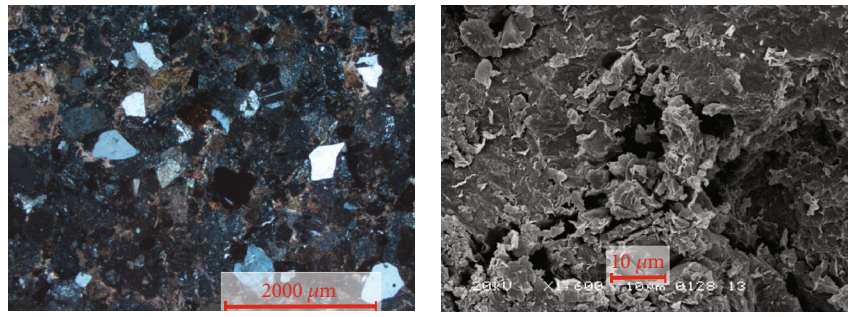

(a) (b)

Figure 4: Microscopic characteristics of carbonate cementation features of sandy conglomerates from Triassic Baikouquan Formation in the slope of the Mahu Sag. (a) The thin-section feature of early calcite crystalline and (b) the scanning electron microscope (SEM) feature of early calcite.

under pressures and occupy the pore and throat space, which degrades the reservoir physical property.

The textural maturity of the sandy conglomerate sample from the study area is also low, with poor sorting and high contents of volcanic lithic fragments and mudstone matrix. Therefore, the development of the early carbonate cementation is suppressed, while such early-diagenesis cementation can support the framework and efficiently reduce the compaction degree during the sediment deposition. In addition, due to the lubricating effects of the mudstone matrix, the clastic sediment is prone to rapid compact, and this stimulates the effects of compaction on the reservoir physical property.

3.2. Cementation. Cementation is an important process, in which sediments are transformed into sedimentary rocks, and it is also one of the main reasons for porosity and permeability reduction in reservoir rocks. The cementation in the study area is of various types, mainly including carbonate cementation, siliceous cementation, authigenic clay mineral cementation, and zeolite cementation.

3.2.1. Carbonate Cementation. Carbonate cements such as calcite, ferrocalcite, and dolomite are extensively developed in the Triassic Baikouquan Formation, and the iron-containing filled among particles or around particles is dominant. The early-formed calcite has low degrees of crystallinity, and the crystalline grain is generally small (Figure 4). The late-formed carbonate cement often has large crystalline grains and usually contains a certain amount of iron. The distribution of the calcite cementation in the study area is relative broad. The calcite often presents porous-type cementation, while the ferrocalcite is in most cases seen as filling the primary or secondary pores in the patch-like, poikilitic, or pore-lining structures.

3.2.2. Siliceous Cementation. In the study area, the siliceous cement mainly occurs on the pore wall, the pore wall between particles, and the dissolved pores inside the particle in the form of quartz overgrowth and authigenic quartz. The pressure solution process, which the Baikouquan Formation experienced, provides part of the siliceous cement. The coexistence of quartz overgrowth and authigenic quartz with feldspar dissolution is often seen in the SEM analysis, which suggests that the feldspar can be dissolved into water and then form the quartz cement in the case of local supersaturation and resultant precipitation. Although the siliceous cement can ease the compaction during the early diagenesis process and maintain part of the primary pores between the quartz overgrowth boundaries, generally speaking, most of the siliceous cements occupy the pore space and reduce the reservoir porosity, which damages the reservoir physical property.

3.2.3. Clay Mineral Cementation. The compositional and textural maturities of the sandy conglomerate reservoir in

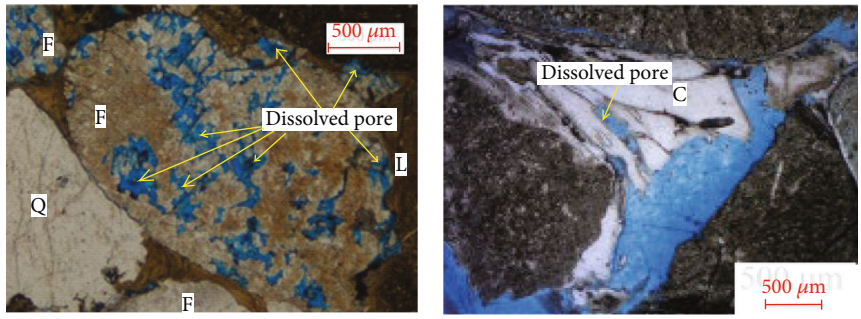

(a) (b)

Figure 5: Microscopic characteristics of dissolution features of sandy conglomerates from Triassic Baikouquan Formation in the slope of the Mahu Sag. In the pictures, pores in blue. (a) A single feldspar has been dissolved and produced many dissolved pores and (b) the cements has been dissolved. F: feldspar; Q: quartz; L: lithics; C: cements.

the Triassic Baikouquan Formation are both relatively low, with high contents of the clay matrix. Hence, the clay minerals are extensively developed in the study area. The X-ray diffraction analysis demonstrates that the clay mineral frequently seen in the study area includes kaolinite, chlorite, mixed layers of illite, and smectite and illite. During the diagenesis process, similar to the carbonate cement, the clay minerals such as the kaolinite, chlorite, and zeolite have double effects upon the reservoir physical property. On the one hand, they occupy part of the primary intergranular and dissolved pores, and thus, to some extent, degrade the reservoir physical property. On the other hand, an appropriate amount of clay mineral and carbonate cements can protect the pores from the compaction during the diagenesis process, especially in the early stage. In the late diagenesis stage, with certain pore fluids and environment media, they can provide the material basis for the late dissolution as the soluble composition.

3.3. Dissolution. There are two stages of large-scale hydrocarbon generation and expulsion in the history of Mahu Sag burial, and a large amount of organic acid would be produced, so the rock of Baikouquan Formation in Mahu Sag would be dissolved that a lot of dissolution has transformed the reservoir. The feldspar and various cements in the rock always be dissolved in the study area. Feldspar-rich shows large-scale dissolution, with feldspar particles displaying intragranular dissolution. Figure 5(a) shows a single feldspar particle with several small intragranular pores, and Figure 5(b) shows the cements were dissolved.

3.4. Sequence of Diagenetic Evolution. The configuration relationships of various clay minerals and the mineral composition of cement were observed to clarify the sequence of diagenetic evolution through different methods, such as core analysis, observation of thin sections, and SEM [25, 26]. Diagenesis is closely related to reservoir depth (Figure 6). At burial depths less than 2000 m (early diagenetic stage), the main pore types are residual intergranular pores, the main diagenesis processes are compaction and cementation, and clay minerals are mainly mixed illite/smectite (I/S) and kaolinite, with a small amount of early calcite cementation and detrital feldspar dissolution. Early oil emplacement is evident, with the primary intergranular pores developed during this stage.

Upon increasing the burial depth, the primary porosity decreases abruptly. When the burial depth reaches 2000-5000 m, the reservoir space is mainly in secondary feldspar-dissolution pores, with a few pores from clay shrinkage and residual intergranular pores. Compared to the shallower depths, the fractions of I/S mixed-layer minerals and kaolinite decreased abruptly, authigenic illite and chlorite gradually increased, and detrital feldspar clearly dissolved. In addition, authigenic quartz cement and oil emplacement are found in feldspar-dissolution pores. Layers are tight where feldspar-dissolution pores are undeveloped, so the development of feldspar dissolution pores improved the physical properties of the reservoir for oil storage, which is likely the reason that the reservoir developed in the Baikouquan Formation. Some of the sandy conglomerate has now been tightened into an oil and gas seal because of differences in rock composition, feldspar content, diagenesis, and diagenetic environment.

4. The Relationship between Elastic Characteristics and Reservoir Property of Sandy Conglomerate in Mahu Sag

4.1. Reservoir Physical Property Characteristics in the Mahu Sag. The study on the reservoir physical property of sandy conglomerates interval of the Triassic Baikouquan Formation in the Mahu Sag indicates that the porosity (ϕ) mainly ranges between 4% and 15%, with an average of 9.7%. The permeability (K) is in the range of 0.078-75.3 mD, while the average permeability is 0.64 mD. A certain correlation is observed between the porosity and permeability (Figure 7), which can to some extent reveal the characteristics of the reservoir physical property and the pore type. For clastic sand reservoirs, good sorting and psephicity often lead to apparent linear correlation between porosity and permeability.

The reservoir of Triassic Baikouquan formation in the Mahu Sag has been through complex diagenesis processes, and the reservoir has high heterogeneity. The linear

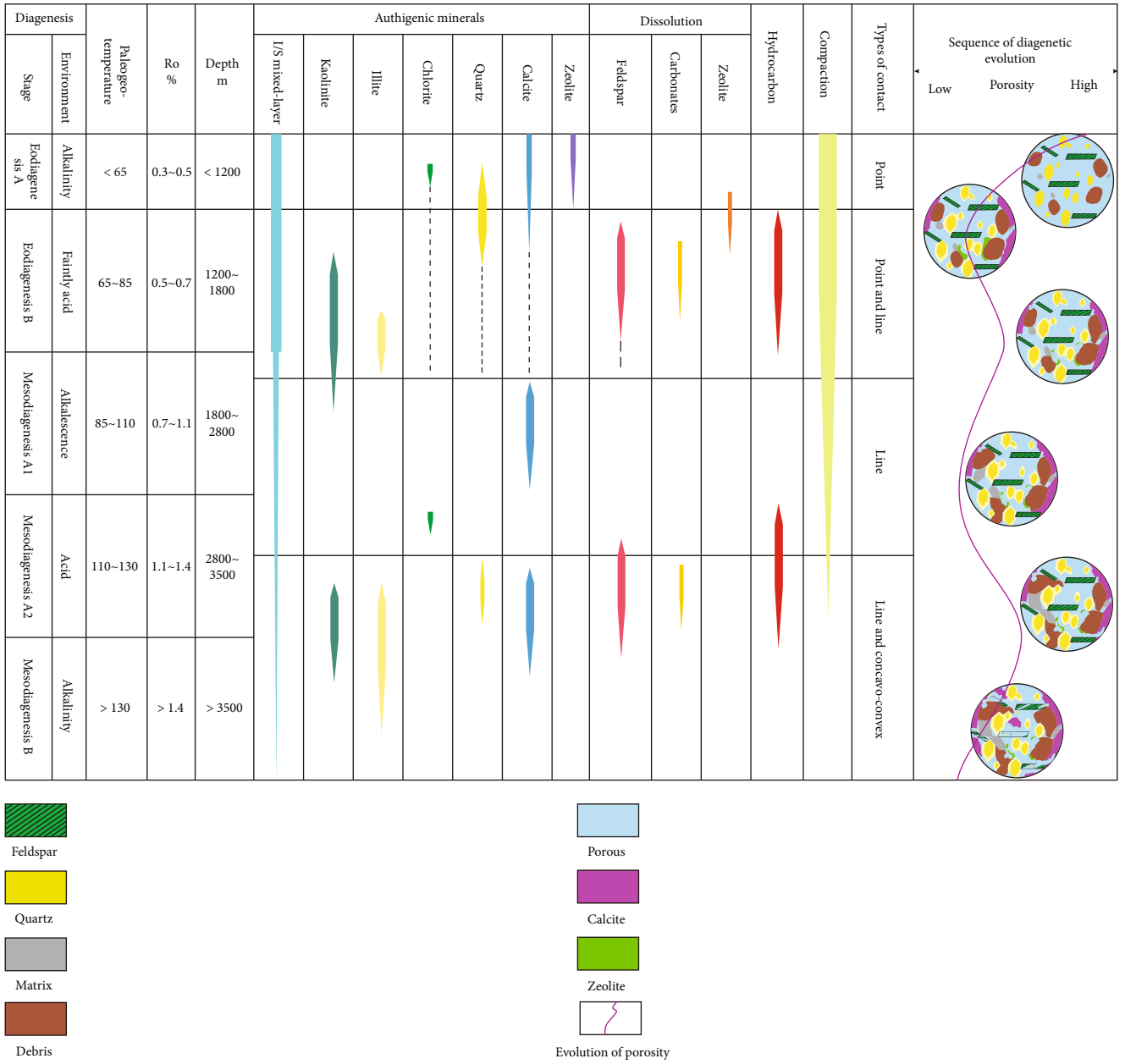

Figure 6: Synthetic diagram showing the diagenetic sequence and porosity evolution of Baikouquan formation in Mahu Sag.

correlation between porosity and permeability is complicated. Dependency of permeability on porosity exists, and yet is relatively low. The dissolution process in the late stage can increase the effective permeability of the rock sample, and the presence of the dissolved pores and crushed crack of grains considerably improve the effective permeability of the rock sample (Figure 8(a)). As for the rock with high contents of plastic lithic fragments, the grains tend to bend under the compression stress, and part of the deformed plastic particles fill between the pores and throats, which negatively impact the general rock physical property (Figure 8(b)). The main type of reservoir space is secondary pore, which mainly includes intragranular dissolution pores, intergranular dissolution pores, and microcracks. The feldspar-rich sandy conglomerate shows large-scale dissolution [27, 28].

4.2. The Relation between Sonic Velocity and Porosity of Reservoirs in the Mahu Sag. Porosity has notable influences upon the elastic characteristics of rock. In fact, the function between the elastic attribute and porosity cannot be built for rock, as a heterogeneous complex medium. However, the correlation between the elastic attribute and rock physical property plays a vital role in the seismic data interpretation, reservoir evaluation, and inversion works. Therefore, simple experimental empirical correlations are often adopted to replace the theoretical relationship. The frequently-used velocity-porosity experimental correlation mainly includes (1) the Wyllie equation (the time average equation), (2) the Raymer equation, and (3) the velocity-porosity-clay-mineral-content correlation [29–31].

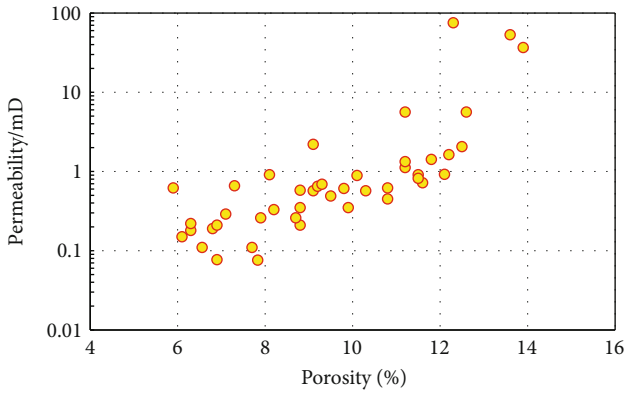

Figure 7: Cross plot of permeability and porosity of rock samples from the study area.

The correlation between the measured P-wave velocity and porosity under the effective pressure $P_{\text{eff}} = 30$ MPa is presented in Figure 9.

It is seen that strong dependencies between P-wave and S-wave velocities and the rock porosity are found (equations (1) and (2)). In the case of the effective pressure of 30 MPa, the correlation coefficients of P-wave and S-wave velocities versus porosity R^2 are 0.63 and 0.64, respectively. Significant differences between the velocity-porosity correlations calculated using the Wyllie (time average) and Raymer equations and the measurements. With a fixed porosity, the calculated P-wave velocity based on the Wyllie equation is greatly higher than the experimental measurement. While the test data of P-wave velocity in most cases surpass the results of the Raymer equation, the measured S-wave velocity is far below the corresponding results of the Raymer equation.

$$Vp = 3.1133\phi^2 - 212.62\phi + 6132.3 \; R^2 = 0.631, \quad (1)$$

$$Vs = -73.752\phi + 3289.7 \; R^2 = 0.6497. \quad (2)$$

Although a good linear correlation is presented between the measured sandy conglomerate sonic velocity and the porosity, the velocity values are still dispersed in the case of middle and high porosity, in which the velocity gap between samples with the same porosity can be over 800 m/s. From the casting thin-section analysis, it is shown that the sample with a low sonic velocity is dominated by the sand having massive intergranular pores and microcracks and presenting a typical quartz-grain-supporting feature (Figure 10(a)). In such cases, many of the primary pores are maintained during the compaction process. As for the sample with the same porosity and yet higher sonic velocity, its pores are dominated by the intragranular pores (Figure 10(b)). The pore type difference resulted from the diagenesis is one of the main contributor to the sonic velocity variation between rock samples. The velocity at zero porosity (namely the mineral spot velocity) is obtained using the fitting formula. The mineral spot velocity of the tested sample is 5643 m/s, while the typical mineral spot velocity of sandy conglomerates lies between 5480 m/s and 5950 m/s. The rock sample calculation result is close to the lower limit of the sandy conglomerate range, which is mainly due to the effects of the clay minerals and calcium cements on the elastic parameters of the reservoir in the study area.

In the case of dry samples, the P-wave and S-wave velocity show apparent positive correlations with the ratio of P-wave and S-wave velocity. That is to say, the higher the P-wave and S-wave velocity are, the higher the corresponding velocity ratio is. This change pattern is clearly related to the diagenetic process of the sandy conglomerate sample. The P-wave velocity of the sample is mainly controlled by the porosity, and the reduction in porosity (especially the primary porosity) is closely related to the compaction process. With massive plastic clastics such as the clay clastics in the sample, the intergranular pores and throats tend to be occupied by those clastics deformed under compaction, and under such circumstances, the porosity rapidly declines and consequently the P-wave velocity grows (Figures 10(a) and 10(c)). The P-wave velocity grows faster than the S-wave velocity, due to the intrinsic elastic property of the clastic grains such as clays filled in the pores. Thus, it can be concluded that for dry rock samples, the P-wave and S-wave velocities both increase with higher contents of plastic clastics such as clays, and so does the ratio of P-wave and S-wave velocity. It is also indicated that the P-wave and S-wave velocity of the tested rock sample are apparently higher than those of conventional sandstone, which can be explained mainly by the effects of plastic clastics such as clay in the sandy conglomerate. In addition, the overpressure also stimulates the ratio of P-wave and S-wave velocity, as it impacts the S-wave velocity.

5. Seismic Petrophysical Modeling

For the rock-physics modeling, the sandy conglomerates can be assumed to be isotropic, which implies that elastic stiffness tensor can be completely defined using the two elastic parameters: bulk modulus K and shear modulus μ. In order to complete the petrophysical modeling of sandy conglomerate in the study area, we divide the porosity evolution into three intervals according to the diagenetic process. The first is a low-porosity interval valid for porosities within $0 \le \phi \le \phi_{\text{max,DEM}}$, where the DEM model is used to predict the elastic properties. Here, $\phi_{\text{max,DEM}}$ defines a preset maximum porosity for which the DEM model is used. This value has to be evaluated in correspondence with the particular pore model being used. A high-porosity ϕ_{CCT} interval is then defined, where the elastic moduli are found using the cementation theoretical model (CCT). Finally, the elastic properties in the middle porosity interval $(\phi_{\text{max,DEM}}, \phi_{\text{CCT}})$ are found using the Hashin-Shtrikman upper bound (HS^+), where the stiff component is defined by the elastic moduli obtained from DEM modeling of the low porosity interval, and those of the soft component are defined at the maximum porosity point using the CCT model. Furthermore, in our approach, the stiff component becomes gradually more porous as the porosity decreases from the maximum porosity point (ϕ_{CCT}) to the highest porosity point of the lowest porosity interval ($\phi_{\text{max,DEM}}$). More details of the three modeling intervals are given below.

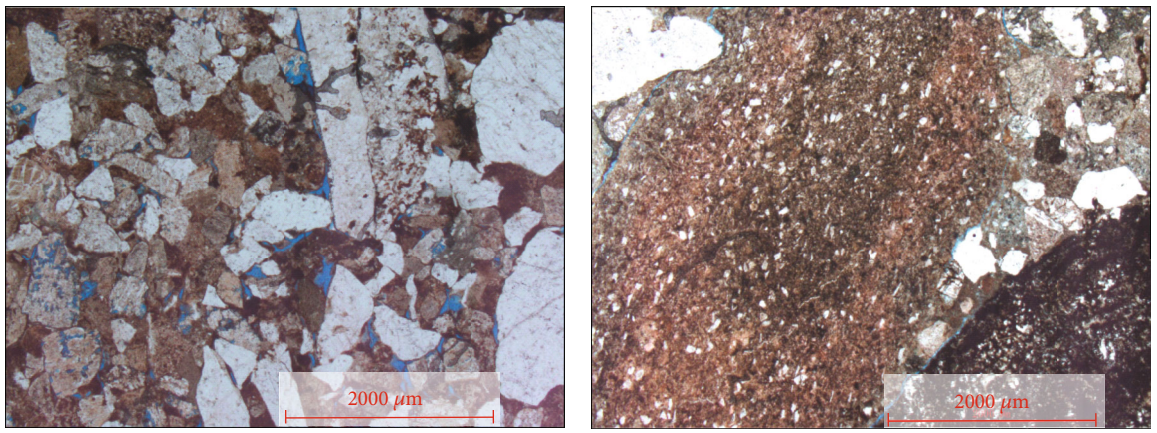

(a) (b)

Figure 8: Reservoir physical property characteristics under varied diagenesis processes. (a) Sample no. 26, well Ma19 ($\phi = 12.3\%$, $K = 75.3$ mD). (b) Sample no. 2, well Ma603 ($\phi = 6.1\%$, $K = 0.15$ mD).

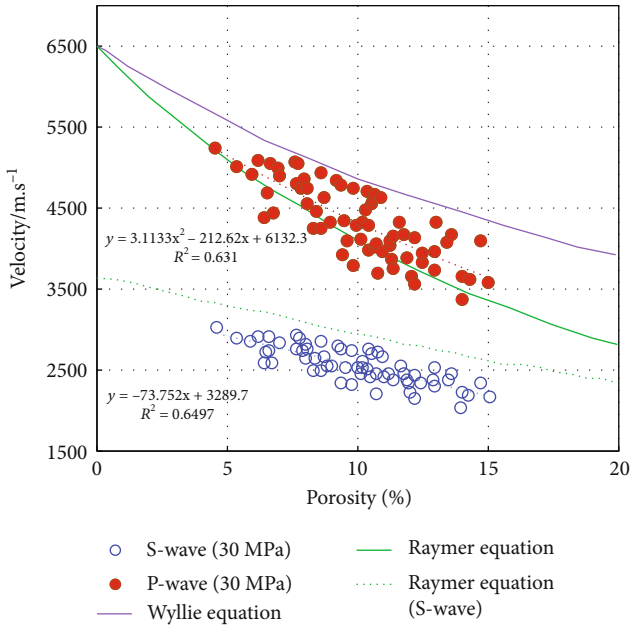

Figure 9: The cross plot between porosity and P-wave and S-wave velocity of sandy conglomerates samples in the study area.

Given the aforementioned, the diagenetic process of the reservoir in the study area mainly includes compaction, cementation, dissolution, and hydrocarbon emplacement. The reservoir depth is of 2800 m-3300 m, and part of the reservoir has been greatly modified by the strong compaction. The reservoir highly impacted by compaction is often the sandy conglomerate with poor sorting, high contents of the muddy matrix, and low contents of carbonate cements. The whole sedimentation-diagenesis geological process has significant effects on the porosity and seismic elasticity of the reservoir rock. The early calcium cementation leads to the preliminary consolidation of the grain aggregate, and the cement "welds" the particle. Accordingly, the rigidity of the rock greatly grows, and the P-wave and S-wave velocity considerably climb up, with only minor change of porosity.

The cementation theoretical model presented by Dvorkin illustrates the mechanical interaction between two rigid particles cemented by elastic cements. In this model, the cement serves as part of the framework to bear the external load, and thus, even a very small amount of cements can lead to notable increase in the rigidity of the particle aggregate [32]. The contact-cement model assumes that the sandstone is originally formed by closely packed quartz grains with the identical size, and the corresponding porosity is the critical porosity ($\phi_0 \approx 40\%$). The continuous porosity reduction of sandstones is due to the fact that cements subsequently stick to the surface of the quartz grains in the late stage, and the effective elastic modulus of sandstones grows. In particular, the initial small amount of cements will cause dramatic growth in the sonic velocity and modulus, with only slight change to the porosity. The calculation equation of the contact-cement model is shown in the following equation:

$$K_{\text{eff}} = \frac{1}{6} n(1 - \phi_0) K_c S_n,$$
$$\mu_{\text{eff}} = \frac{3}{5} K_{\text{eff}} + \frac{3}{20} n(1 - \phi_0) \mu_c S_\tau, \quad (3)$$

where K_{eff} and μ_{eff}, respectively, stand for the effective bulk and shear moduli of the dry cemented mineral aggregate; K_c and μ_c are the bulk and shear moduli of the cement, respectively; S_n and S_τ are statistical elastic parameters related to the rock rigidity.

Since the clastic rock in the Mahu Sag is poorly sorted, during the modeling of the clastic rock in the Mahu Sag on the basis of the experimental data, the critical porosity is set as $\phi \approx 35\%$, the content of the calcium cement is 5%, and other elastic parameters are shown in Table 1. The dissolution process also greatly influences the porosity of the reservoir sandstone, and its impacts on the elastic wave velocity mainly work jointly via the porosity and the pore shape. In the case of zero porosity of the sandstone reservoir after compaction and later chemical cementation, a certain additional porosity of ϕ resulted from the dissolution.

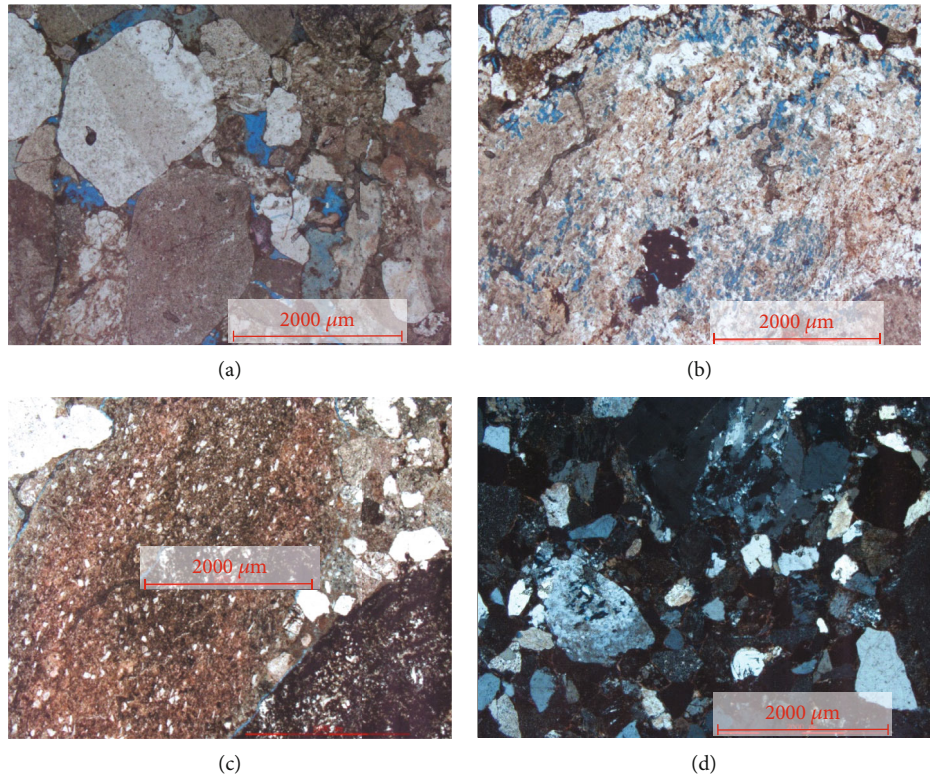

Figure 10: Thin-section features corresponding to elastic parameters and physical properties of tested samples under different diagenetic conditions. (a) Sample no. 18, well Ma19 ($V_p = 3.6$ km/s, $\phi = 14.3\%$). (b) Sample no. 5, well Ma18 ($V_p = 4.1$ km/s, $\phi = 14.7\%$). (c) Sample no. 2, well Ma603 ($V_p = 5.0$ km/s, $\phi = 6.1\%$). (d) Sample no. 69, well Ma15 ($V_p = 4.36$ km/s, $\phi = 6.41\%$).

Table 1: Elastic parameters of minerals.

Mineral name	Bulk modulus (GPa)	Shear modulus (GPa)	Poisson's ratio
Quartz	39	44	0.06
Feldspar	37.5	15	0.32
Clay	17.5	7.5	0.33
Calcite	76.8	32	0.32

Taking the shape of the pore into consideration, the differential effective medium (DEM) model calculates the seismic elastic property variation from zero porosity to porosity of ϕ. The DEM model can be described as below:

$$\begin{aligned}(1-\phi)\frac{d}{d\phi}[K_{\mathrm{DEM}}(\phi)] &= [K_f - K_{\mathrm{DEM}}(\phi)]P^*(\phi),\\ (1-\phi)\frac{d}{d\phi}[\mu_{\mathrm{DEM}}(\phi)] &= -\mu_{\mathrm{DEM}}(\phi)Q^*(\phi),\end{aligned} \tag{4}$$

where $K_{\mathrm{DEM}}(\phi)$ and $\mu_{\mathrm{DEM}}(\phi)$ are the effective bulk and shear moduli, respectively, and starting from initial conditions $K_{\mathrm{DEM}}(\phi = 0) = K_s$ and $\mu_{\mathrm{DEM}}(\phi = 0) = \mu_s$, which in our case is set to the elastic moduli of the mineral. P^* and Q^* are geometrical factors associated with the aspect ratios of the pores.

In the practical calculation process, it is assumed that the microcracks would be randomly distributed in the rock, and the whole rock medium is isotropic. The elastic feature of rock with isolated pores estimated through the DEM method is applicable to high-frequency cases of saturated pores with no fluid flow [33].

The reservoir compaction mainly occurs after the early calcium cementation and has apparent effects on both the rock porosity and seismic elastic. The Hashin-Shtrikman elastic upper bound corrected using the critical porosity is used to connect the early calcium cementation scenario with the dissolved pore scenario. The Hashin-Shtrikman elastic upper bound is expressed as below:

$$\begin{aligned}K &= \left[\frac{1-\phi/\phi_0}{K_0 + (4/3)\mu_{\mathrm{SS}}} + \frac{\phi/\phi_0}{K_{\mathrm{SS}} + (4/3)\mu_{\mathrm{SS}}}\right]^{-1} - \frac{4}{3}\mu_{\mathrm{SS}},\\ \mu &= \left(\frac{1-\phi/\phi_0}{\mu_0 + Z_{\mathrm{SS}}} + \frac{\phi/\phi_0}{\mu_{\mathrm{SS}} + Z_{\mathrm{SS}}}\right)^{-1} - Z_{\mathrm{SS}},\\ Z_{\mathrm{SS}} &= \frac{\mu_{\mathrm{SS}}}{6}\frac{9K_{\mathrm{SS}} + 8\mu_{\mathrm{SS}}}{K_{\mathrm{SS}} + 2\mu_{\mathrm{SS}}},\end{aligned} \tag{5}$$

where K_0 and μ_0 are the effective bulk and shear moduli of sandy conglomerates with minimum porosity, respectively. K_{ss} and μ_{ss} are the effective bulk and shear moduli of sandy conglomerates with critical porosity, respectively.

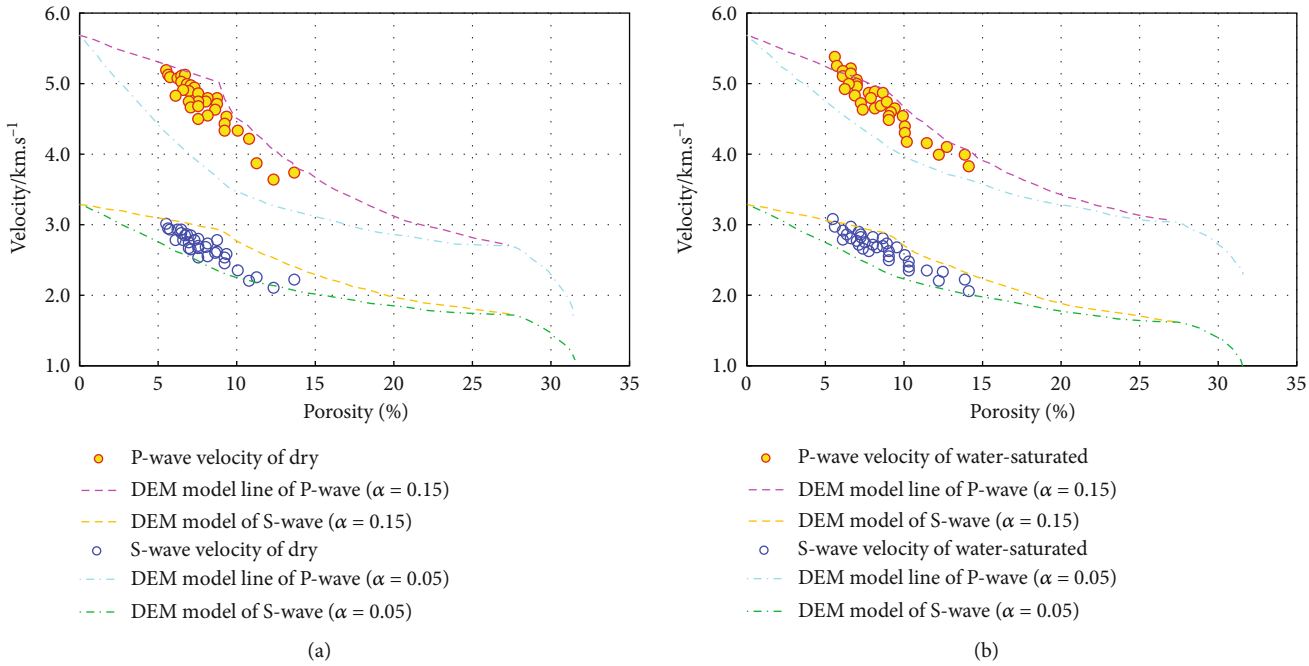

Figure 11: The cross plot of sonic velocity and porosity, Baikouquan sandy conglomerate reservoirs.

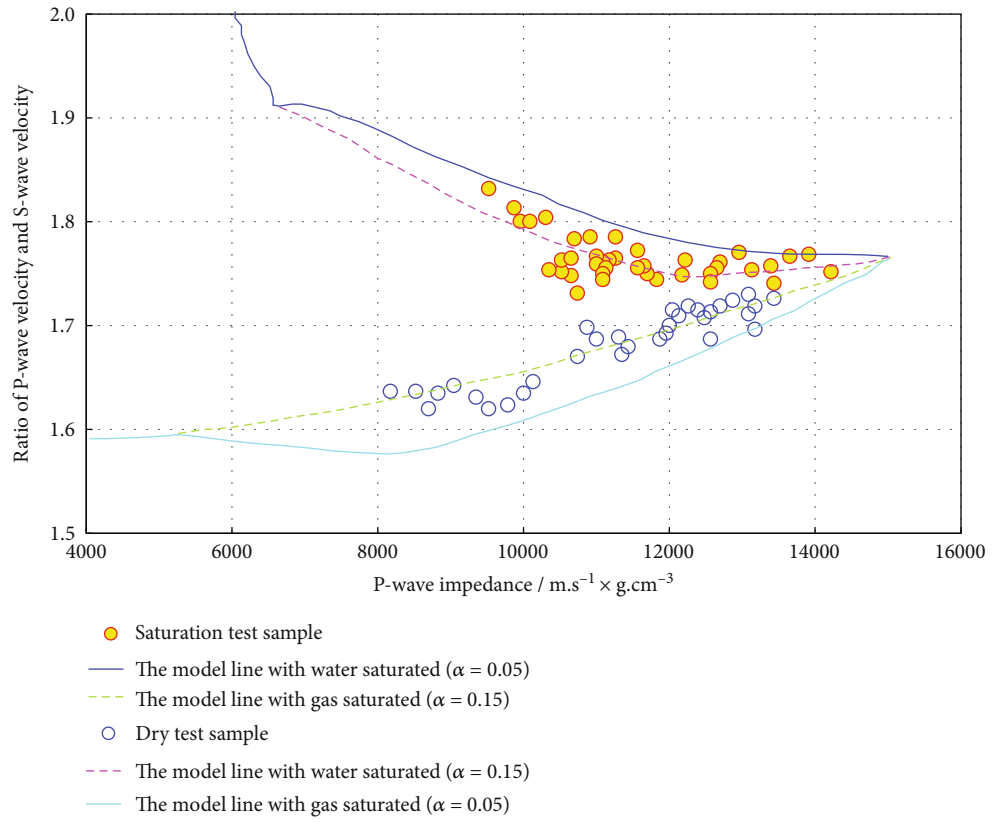

Figure 12: The Baikouquan sandy conglomerate reservoirs relation between P-wave impedance and the ratio of P-wave and S-wave velocity.

The P-wave and S-wave velocities of dry (Figure 11(a)) and water-saturated (Figure 11(b)) sandy conglomerate samples are measured and presented in Figure 11. The velocity-porosity correlation presented by the test data is consistent with tendency shown by the theoretical calculation results. The DEM model with a pore aspect ratio α = 0.05 can give the lower bound of the experimental data, while the model with $\alpha = 0.15$ complies with the

approximate of the upper bound of the experiment data. This suggests that the average pore aspect ratio of the test sample lies between 0.05 and 0.15, indicating dissolve pore characteristics with the relative "rigid" elastic property. The water-saturated velocity and porosity calculated from the Gassmann equation can also consistently interpret the test data, and so can the theoretical variation of the P-wave impedance with the ratio of P-wave and S-wave velocity based the proposed model (Figure 12).

6. Conclusions

(1) The sandy conglomerate of Baikouquan Formation in Mahu Sag has experienced a complex diagenetic evolution process. Affected by different diagenesis, the sandy conglomerate is highly heterogeneous, and its physical properties change greatly. Dissolution has the strongest constructive effects, and compaction has the strongest negative effects upon the reservoir physical property in the study area. To quantitatively characterize the influence of different diagenesis on rock physical properties, we have established a rock-physics modeling strategy that combines the contact-cement model with the differential effective medium model and Hashin-Shtrikman upper bound

(2) The modeling approach takes into account the burial history of the sandy conglomerate of Baikouquan Formation in Mahu Sag and successfully predicts the rock-physics and seismic properties as a function of rock texture and pore fluid characteristics of these sandy conglomerate. We also can use the model to better understand the seismic signature of the studied Mahu sandy conglomerate reservoirs or other low-to-intermediate-porosity reservoirs elsewhere

Abbreviations

V_p: P-wave velocity (m/s)
V_s: S-wave velocity (m/s)
ϕ: Porosity (%)
K: Bulk modulus (GPa)
μ: Shear modulus (GPa)
n: The average number of contacts per grain
S_n: The normal stiffness
S_τ: The shear stiffness
P^*: Geometrical factors associated with the aspect ratios of the pores
Q^*: Geometrical factors associated with the aspect ratios of the pores.

Data Availability

The data used to support the findings of this study are corrected and included within the article.

Conflicts of Interest

The authors declare that they have no conflicts of interest.

Acknowledgments

The authors sincerely thank Wang Xiaojun, Tang Yong, Qu Jianhua et al. from the Xinjiang Oilfield Company, PetroChina, for their great support during this research. This study was supported by the National Natural Science Foundation of China (Grant nos. 41574103, 41974120, 41774130, and U20B2015).

References

[1] F. Chen, X. Wang, and X. Wang, "Prototype and tectonic evolution of the Junggar basin, northwestern China," *Earth Science Frontiers*, vol. 12, no. 3, pp. 77–89, 2005.

[2] S. F. Zhu, X. M. Zhu, Y. B. Wang et al., "Dissolution characteristics and pore evolution of Triassic reservoir in Ke-Bai area, northwestern margin of Junggar Basin," *Acta Sedimentologica Sinica*, vol. 28, no. 3, pp. 547–555, 2010.

[3] S. C. Zhang, Z. J. Huang, X. C. Lu et al., "Main controlling factors of Permian sandy conglomerate reservoir in the northwestern Junggar Basin," *Journal of Lanzhou University (Natural Sciences)*, vol. 51, no. 1, pp. 20–30, 2015.

[4] L. C. Kuang, Y. Tang, D. W. Lei, T. Wu, and J. H. Qu, "Exploration of fan-controlled large-area lithologic oil reservoirs of Triassic Baikouquan Formation in slope zone of Mahu Depression in Junggar Basin," *China Petroleum Exploration*, vol. 19, no. 6, pp. 14–23, 2014.

[5] J. Jin, X. Kang, W. X. Hu, B. L. Xiang, J. Wang, and J. Cao, "Diagenesis and its influence on coarse clastic reservoirs in the Baikouquan Formations of western slope of the Mahu Depression, Junggar Basin," *Oil & Gas Geology*, vol. 38, no. 2, pp. 323–406, 2017.

[6] K. J. Tan, G. D. Wang, H. F. Luo, Y. Q. Qu, L. Yin, and J. Chen, "Reservoir characteristics and controlling factors of the Triassic Baikouquan Formation in Mahu slope area, Junggar Basin," *Lithologic Reservoirs*, vol. 26, no. 6, pp. 83–88, 2014.

[7] H. Zhou, J. A. Shi, Y. Tang, C. Ding, and S. C. Zhang, "Characteristics of diagenesis and diagenetic facies of Permian clastic reservoir in northwest margin of Junggar Basin," *Acta Sedimentologica Sinica*, vol. 29, no. 6, pp. 1069–1078, 2011.

[8] Z. W. Zhou, H. Li, Y. Xu, C. F. Yu, and X. C. Meng, "Sedimentary characteristics of the Baikouquan Formation, lower Triassic in the Mahu Depression, Junggar Basin," *Bulletin of Geological Science and Technology*, vol. 34, no. 2, pp. 20–26, 2015.

[9] Y. Kuang, L. Q. Sima, J. H. Qu, D. N. Wen, M. Chen, and F. Chen, "Influencing factors and quantitative evaluation for pore structure of tight glutenite reservoir: a case of the Triassic Baikouquan Formation in Ma 131 well field, Mahu Sag," *Lithologic Reservoirs*, vol. 29, no. 4, pp. 91–100, 2017.

[10] X. Shan, N. G. Chen, H. J. Guo et al., "Reservoir evaluation of sand conglomerate reservoir based on petrophysical facies: a case study on Bai 2 reservoir in the Ma131 region, Junggar Basin," *Acta Sedimentologica Sinica*, vol. 34, no. 1, pp. 149–157, 2016.

[11] Y. Chen, L. M. He, Z. G. Cheng, and J. H. Tang, "The research and application of prestack seismic prediction in high quality

glutenite reservoir in the western Mahu slope of Junggar Basin," *Xinjiang Geology*, vol. 34, no. 2, pp. 291–296, 2016.

[12] J. H. Qu, R. R. Yang, and Y. Tang, "Large-area petroleum accumulation model of the Triassic glutenite reservoirs in the Mahu Sag, Junggar Basin: triple controls of fan, fault and overpressure," *Acta Geologica Sinica*, vol. 93, no. 4, pp. 915–927, 2019.

[13] P. L. Li, *Petroleum Geology and Exploration of Continental Fault Basin*, Petroleum Industry Press, Beijing, 2003.

[14] Y. Hu, H. M. Liu, and X. F. Hao, "The orderly distribution and difference enrichment of glutenite oil and gas in steep slope zone of rift basin: a case study of Dongying Sag, Jiyang Depression, Bohai Bay Basin," *Geological Review*, vol. 67, no. S1, pp. 95-96, 2019.

[15] F. Sui, "Characteristics of reservoir dynamic on the sand-conglomerate fanbodies in the steep-slope belt of continental fault basin: a case study on Dongying depression," *Oil & Gas Geology*, vol. 24, no. 4, pp. 335–340, 2003.

[16] J. Dvorkin, G. Mavko, and A. Nur, "The effect of cementation on the elastic properties of granular material," *Mechanics of Materials*, vol. 12, no. 3-4, pp. 207–217, 1991.

[17] J. G. Berryman, "Long-wavelength propagation in composite elastic media I. Spherical inclusions," *Journal of Acoustical Society of America*, vol. 68, no. 6, pp. 1809–1819, 1980.

[18] M. R. Wyllie, A. R. Gregory, and G. H. Gardner, "An experimental investigation of factors affecting elastic wave velocities in porous media," *Geophysics*, vol. 23, no. 3, pp. 459–493, 1958.

[19] P. Avseth, T. A. Johansen, A. Bakhorji, and H. Mustafa, "Rock-physics modeling guided by depositional and burial history in low-to-intermediate-porosity sandstones," *Geophysics*, vol. 79, no. 2, pp. D115–D121, 2014.

[20] H. B. Jia, H. C. Ji, X. W. Li, H. Zhou, L. S. Wang, and G. Yan, "A retreating fan-delta system in the Northwestern Junggar Basin, northwestern China—characteristics, evolution and controlling factors," *Journal of Asian Earth Sciences*, vol. 123, pp. 162–177, 2016.

[21] Y. Tang, Y. Xu, J. H. Qu, X. C. Meng, and Z. W. Zhou, "Fan-Delta group characteristics and its distribution of the Triassic Baikouquan Reservoirs in Mahu Sag of Junggar Basin," *Xinjiang Petroleum Geology*, vol. 35, no. 6, pp. 628–635, 2013.

[22] Z. Y. Lei, B. Lu, Y. J. Yu, L. P. Zhang, and X. Shi, "Tectonic evolution and development and distribution of fans on northwestern edge of Junggar Basin," *Oil & Gas Geology*, vol. 26, no. 1, pp. 86–91, 2005.

[23] Y. J. Yu, D. S. Li, S. Y. Hu, Z. Y. Lei, and D. F. He, "Fans sedimentation and exploration direction of fan hydrocarbon reservoirs in foreland thrust belt of the northwestern Junggar Basin," *Acta Geoscientica Sinica*, vol. 28, no. 1, pp. 62–71, 2007.

[24] S. C. Zhang, N. N. Zou, J. A. Shi, Q. S. Chang, X. C. Lu, and B. Chen, "Depositional model of the Triassic Baikouquan Formation in Mabei area of Junggar Basin," *Oil & Gas Geology*, vol. 36, no. 4, pp. 640–649, 2015.

[25] J. G. Pan, G. D. Wang, Y. Q. Qu et al., "Origin and charging histories of diagenetic traps in the Junggar Basin," *AAPG Bulletin*, vol. 105, no. 2, pp. 275–307, 2021.

[26] X. B. Zhao, G. Q. Yao, X. Chen, R. Zhang, Z. Lan, and G. Wang, "Diagenetic facies classification and characterization of a high-temperature and high-pressure tight gas sandstone reservoir: a case study in the Ledong area, Yinggehai Basin," *Marine and Petroleum Geology*, vol. 140, article 105665, 2022.

[27] Q. Jia, D. Liu, Y. Cai, Y. Zhou, Z. Zhao, and Y. Yang, "AFM characterization of physical properties in coal adsorbed with different cations induced by electric pulse fracturing," *Fuel*, vol. 327, article 125247, 2022.

[28] Q. Jia, D. Liu, Y. Cai et al., "Nano-CT measurement of pore-fracture evolution and diffusion transport induced by fracturing in medium-high rank coal," *Journal of Natural Gas Science and Engineering*, vol. 106, article 104769, 2022.

[29] J. X. Deng, Z. Y. Tang, Y. Li, J. Xie, H. L. Liu, and W. Guo, "The influence of the diagenetic process on seismic rock physical properties of Wufeng and Longmaxi Formation shale," *Chinese Journal of Geophysics*, vol. 61, no. 2, pp. 659–672, 2018.

[30] J. X. Deng, S. X. Wang, and S. J. Li, "Effects of variations of reservoir sandstone sedimentary characteristics on seismic elastic attributes," *Journal of Oil and Gas Technology*, vol. 30, no. 1, pp. 75–79, 2008.

[31] Z. Q. Song, C. Jing, Y. D. Pang, X. Tian, and J. H. Zhang, "Porosity estimation of tight reservoirs based on petrophysical facies classification: a case study from the east area of the Sulige Gas Field, Ordos Basin," *Natural Gas Industry*, vol. 33, no. 8, pp. 31–37, 2013.

[32] J. Dvorkin, A. Nur, and H. Z. Yin, "Effective properties of cemented granular materials," *Mechanics of Materials*, vol. 18, no. 4, pp. 351–366, 1994.

[33] B. Wang, X. Z. Chen, J. Chen, K. J. Tan, and J. Yao, "Elastic characteristics and petrophysical modeling of the Jurassic tight sandstone in Sichuan Basin," *Chinese Journal of Geophysics*, vol. 63, pp. 4528–4539, 2020.